RSC Advances

ROYAL SOCIETY OF CHEMISTRY

www.rsc.org/advances

RSC Advances

ARTICLE

A green way to increase yield and quality of bio-oil: ultrasonic pretreatment of biomass and catalytic upgrading of bio-oil over metal (Cu, Fe and/or Zn)/γ-Al_2O_3

Received 00th January 20xx,
Accepted 00th January 20xx

DOI: 10.1039/x0xx00000x

www.rsc.org/

Surachai Karnjanakom,[a] Guoqing Guan,[a,b*] Bayu Asep,[a] Xiao Du,[a,c] Xiaogang Hao,[c] Jingxuan Yang,[a,c] Chanatip Samart[d] and Abuliti Abudula[a,b]

A green way is developed to increase yield and quality of bio-oil by ultrasonic pretreatment of biomass followed by in-situ catalytic upgrading of bio-oil over metal (Cu, Fe and/or Zn)/γ-Al_2O_3. It is found that the yield of bio-oil is increased up to [illegible] wt.% after cedar is pretreated by ultrasound before pyrolysis. Various metals (Cu, Fe and Zn) are loaded on γ-Al_2O_3 and applied for the upgrading bio-oil derived from the pyrolysis of pretreated cedar. It is found that the catalysts promote the conversion of oxygenated compounds into aromatic and aliphatic hydrocarbons. Especially, it is favored to produce the monocyclic aromatic hydrocarbons such as benzene and toluene. The best catalytic activity is achieved by using 2.5 wt.% Zn/γ-Al_2O_3 with a maximum hydrocarbon yield of 80.3%. The catalyst is reused up to four cycles. The results show that the catalysts after regeneration by calcination at 550 °C for 30 min exhibits a long-term stability for upgrading of bio-oil.

1 Introduction

Biomass is renewable energy source as eco-friendly energy when compare with conventional energy sources. In general, biomass can combusted directly to provide energy. However, the energy efficiency is not high. To utilize biomass more efficiently, various thermochemical conversion technologies such as torrefaction, gasification, and pyrolysis have been developed.[1-3] Among them, pyrolysis is considered as one of the most promising technologies for bio-oil production.[4,5] It is usually carried out under atmospheric pressure and absence of oxygen at intermediate temperatures ranged from about 300 to 600 °C. Biomass contains three types of macromolecules, i.e., cellulose, hemicellulose and lignin.[6] However, due to its complex and recalcitrant, the yield of bio-oil via pyrolysis process is not so high and the pyrolysis conditions are strict. To enhance the decomposition rate and promote the yield of bio-oil, pretreatment of biomass before reaction is necessary. To date, some pretreatment methods such as organic/inorganic acid and base treatment, and ionic liquid treatment have been developed.[7-10] However, these methods have high cost of disposal and recycling. Especially, a large amount of expensive chemicals are required. To solve these problem and promote pyrolysis efficiency, ultrasonic pretreatment of biomass as a green method has been developed for the destruction of biomass structure, for examples, destroying wax and lignin layers in biomass and breaking the connecting glycosidic bonds.[11] In this study, this method will be applied for pretreating cedar to increase the yield of bio-oil during the pyrolysis process.

On the other hand, the bio-oil produced from pyrolysis without catalyst always contains large amount of oxygenated compounds, which will cause negative properties such as low stability, high corrosiveness and low heating value.[12-14] For instance, the acidic components in the bio-oil could lead to the corrosion of reactor and make the oil unstable.[15] Thus, upgrading of bio-oil is necessary. The conventional bio-oil upgrading method is hydrogen treatment of the oil.[16] However, due to high oxygen content and instability of bio-oil, this method suffers high operating cost together with substantial hydrogen consumption and significant deactivation of the expensive catalysts. Therefore, catalytic upgrading of the bio-oil is required. There are many ways to improve the bio-oil quality including catalytic cracking, decarboxylation, decarbonylation, oligomerization and dehydrogenation with the assistance of various catalysts such as HZSM-5, Al-MCM-41, TiO_2, ZrO_2 and Al_2O_3.[17-23] Mihalcik *et al.*[24] reported that zeolite can effectively promote catalytic cracking reaction during pyrolysis, resulting in hydrocarbon-rich compounds. They found that HZSM-5 shows the most effective in production of aromatic hydrocarbon from the pyrolysis of biomass when compared with other kinds of zeolites. Lu *et al.*[25] found that ZrO_2 and TiO_2 supported catalysts can reduce phenols, sugars and acids in bio-oil significantly while increase the contents of hydrocarbons, cyclopentanones and ketones in the bio-oil. Kaewpengkrow *et al.*[26] reported that Al_2O_3 and TiO_2 (anatase) supported catalysts have the most effective for hydrocarbon production from bio-oil. They considered that the high surface area and large pore size of catalyst can allow the oxygenated compounds easily diffused into the pores and promote the formation of hydrocarbon products in the channels through deoxygenation reactions. Stephanidis *et al.*[27] found that silicalite and Al-MCM-41 supported catalysts have effective for sugar removal from bio-oil with an increasing of polycyclic aromatic hydrocarbons (PAH).

[a] Graduate School of Science and Technology, Hirosaki University, 1-Bunkyocho, Hirosaki 036-8560, Japan.
[b] North Japan Research Institute for Sustainable Energy (NJRISE), Hirosaki University, 2-1-3, Matsubara, Aomori 030-0813, Japan. E-mail: guan@hirosaki-u.ac.jp; Fax: +81-17-735-5411; Tel: +81-17-762-7756
[c] Department of Chemical Engineering, Taiyuan University of Technology, Taiyuan 030024, China.
[d] Department of Chemistry, Faculty of Science and Technology, Thammasat University, Pathumtani 12120 Thailand.

Various metal catalysts such as Ni, Co, Cu, Zn, Pt, Pd and Ru have been applied for the deoxygenation reactions.[28] Liu *et al.*[29] directly loaded Cu on sawdust biomass by impregnation method and found that the sawdust can be decomposed into small-molecular aromatics and the fractions of C_7-C_{10} compounds in the bio-oil are increased significantly. However, Collard *et al.*[30] considered that impregnation of metal in biomass results in the rearrangement reaction occurred, leading to an increase in char product and a decrease in bio-oil formation. In addition, catalyst recovery is difficult in this case. In fact, loading metals on support materials by impregnation method has many advantages such as low production cost, high catalytic activity and high stability.[31,32] French and Czernik[33] loaded Ni, Co, Fe and Ga ZSM-5 and found that hydrocarbon yield increased to a great extent. However, they also found coke deposition on catalyst decreased the deoxygenation activity. Yu *et al.*[21] incorporated metal (metal= La, Ni and Fe) in Al-MCM-41 for effective deoxygenation bio-oil. Recently, γ-Al_2O_3 has been applied as catalyst support for bio-oil upgrading due to its high surface area (>200 m^2/g), large pore size (>5nm) and high acidity (>0.3 mmol/g). The acid site of catalyst has been found to promote deoxygenation reaction via carbonium ion mechanism. Large pore size of γ-Al_2O_3 provides the potential for the diffusion of the large molecules, particularly with lignin-derived compounds. Imran *et al.*[34] investigated alumina-supported sodium carbonate for the catalytic flash pyrolysis of biomass, and found that Na_2CO_3/γ-Al_2O_3 shows high effectivity for the oxygen removal from bio-oil and the acid components in bio-oil can be completely eliminated. Moreover, the coke formation can be effectively reduced due to its large pore size. Especially, when Zn is loaded on the support, the catalytic activity can be promoted and a long-term stability remained since coke formation can be effectively prevent over protons during the reaction.[35] In this study, three kinds of metals, i.e., Cu, Fe and Zn, are loaded on γ-Al_2O_3 and applied for upgrading of bio-oil derived from the pyrolysis of ultrasonic pretreated cedar wood. As-prepared catalysts are characterized by BET, XRD, NH_3-TPD and SEM-EDX. The catalyst reusability is also investigated. It is expected that the yield of bio-oil together with its quality can be promoted by using this process.

2 Experimental

2.1 Biomass materials

Cedar wood was collected from Aomori, Japan and used as biomass feedstock in this study. It is crushed and sieved with a size in a range of 1-2.8 mm and dried at 105 °C. Proximate analysis such as moisture, volatile matter, ash and fixed carbon in cedar wood was determined according to ASTM D7582 standard. Ultimate analysis was carried out to determine the elemental composition (C, H, N, S and O) by using an elemental analyzer (Vario EL cube elemental analyzer). Ash composition was analyzed using an energy dispersive X-ray spectrometer (EDX-800HS, Shimadzu, Japan). The results of proximate, ultimate and ash composition are shown in Table 1.

2.2 Pretreatment of biomass by ultrasound

2 g of cedar wood was moistened with 50 mL of distilled water, conducted in an ultrasonic bath (USD-1R, AS ONE) under a frequency of 40 kHz and a power of 150 W for 2 h. After that, the mixture solution was evaporated at 80 °C for removal of water and then dried at 105 °C overnight in oven.

Table 1 Proximate, ultimate and ash compositions of cedar wood

Biomass	Cedar wood
Proximate analysis (wt.%)[a]	
Volatile matter	86.9
Ash	0.6
Fixed carbon[b]	12.5
Ultimate analysis (wt.%)[c]	
Carbon	48.8
Hydrogen	6.6
Nitrogen	1.4
Sulfur	0.2
Oxygen[b]	43.0
Ash composition analysis (wt.%)	
K_2O	4.01
CaO	50.68
P_2O_5	6.45
SO_3	10.47
SrO	0.04
SiO_2	6.83
Fe_2O_3	0.80

[a] Dry basis; [b] Mass difference; [c] Dry and ash-free

2.3 Catalyst preparation

Metal (Cu, Fe and Zn) loading on γ-Al_2O_3 (Alfa Aesar, Japan) was performed by impregnation method. Before impregnation, γ-Al_2O_3 was calcined at 600 °C for 6 h under air atmosphere. In a typical impregnation process, a certain amount of γ-Al_2O_3 was added into $Cu(NO_3)_2.3H_2O$, $Fe(NO_3)_2.9H_2O$ and/or $Zn(NO_3)_2.6H_2O$ (Wako, Japan) solution and stirred at ambient temperature for 2 h. Then, the slurry was dried at 80 °C for water evaporation and then calcined in air at 550 °C for 4 h in air atmosphere. For comparison, SiO_2 (Saint-Gobain, Norpro, Japan) was also selected as support and metal (Cu, Fe and Zn) loading on it was performed by the same impregnation method.

2.4 Catalyst characterization

Specific BET surface area, pore volume and pore diameter of catalyst were determined by N_2 adsorption-desorption using a Quantachrome instrument (NOVA 4200e, USA). Crystalline structure of catalyst was examined by a X-ray diffractometer (XRD, Rigaku Smartlab, Japan) in the 2θ range of 20 to 90° with a scanning step of 0.02° using Cu Kα radiation (λ = 0.1542 nm). Acidity of catalyst was determined by NH_3-Temperature-programmed desorption (NH_3-TPD) using a BET-CAT catalyst analyzer (BEL, Japan). The surface morphology of catalyst was observed with a scanning electron microscope (SEM, SU8010, Hitachi, Japan) coupled with energy dispersive X-ray detector (EDX). The amount of coke deposition on catalyst was determined using a thermogravimatric analyzer (TGA, DTG-60H, Shimadzu, Japan) with a heating rate of 10 °C/min to a temperature of 800 °C under air flow.

2.5 Catalytic upgrading experiment

All experiments were carried out in a fixed bed reactor using Ar flow (50 cm^3/min) as carrier gas. The schematic diagram of the experimental setup was described in details elsewhere.[36] Before starting the experimental reaction, Ar gas was flowed into the reactor for about 15 min to move out the inside air. In a typical run,

0.6 g of biomass and 2 g of catalyst were separately packed by the quartz wool in the reactor. The pyrolysis reaction temperature, reaction time and heating rate were fixed at 500 °C, 30 min and 20 °C/min, respectively. The bio-oil product was trapped by acetone in ice-cooling bottle and the non-condensed gas was purified and collected in a gas bag for further analysis.

2.6 Analysis of bio-oil and gas products

The collected bio-oil was analyzed with a gas chromatography (GC-2010 Plus, Shimadzu, Japan)/mass spectrometry (GCMS-QP2010 Ultra, Shimadzu, Japan) with Ultra ALLOY$^+$ -5 capillary column. The bio-oil was injected using auto injection mode into the column where the temperature was increased from 50 to 300 °C with a ramp rate 10 °C/min and hold at 300 °C for 10 min. The ionization chamber of MS setup was set at 200 °C. Various peaks in chromatogram corresponding to various compounds such as aromatic, aliphatic, phenol, ketone, aldehyde, furan, sugar and acid were identified by comparison with the built-in NIST spectral library. The water content in bio-oil was measured using Karl-Fisher Titration method (MKS-500, KEM, Japan). The collected non-condensed gas was analyzed off-line using a gas chromatography (Agilent 7890A GC system, USA) equipped with thermal conductivity detector (TCD) and 3 packed columns (1 molecular sieve 5A column + 1 HayeSep Q column + 1 molecular sieve 5A column) for separation of CO, CH_4 and CO_2 using He as a carrier gas, while a molecular sieve 5 A for H_2 detection using Ar as a carrier gas.

3 Results and Discussion

3.1 Characterization of catalyst before reaction

As shown in Table 2, BET surface areas and pore diameters of all catalysts slightly decrease after the metal loading, indicating that metal particles should be dispersed, covered and occupied on the surface and the pores of γ-Al_2O_3. The metal amount on catalyst surface is estimated by EDX. The catalysts are found to have metal amount about 2.5 wt.% on its surface which corresponds with calculated metal loading amount by preparing impregnation method. Fig. 1 shows XRD patterns of metal loaded γ-Al_2O_3. For 2.5 wt.% of metal loading on γ-Al_2O_3, one can see that no diffraction peaks attribute to Cu, Fe and Zn species, indicating that the metal oxide size is small and well dispersed in γ-Al_2O_3.[37] However, the diffraction peaks of CuO, FeO and ZnO crystalline phase are observed for 10 wt.% of metal loading on γ-Al_2O_3, resulting from more crystallite growth and lower dispersion.

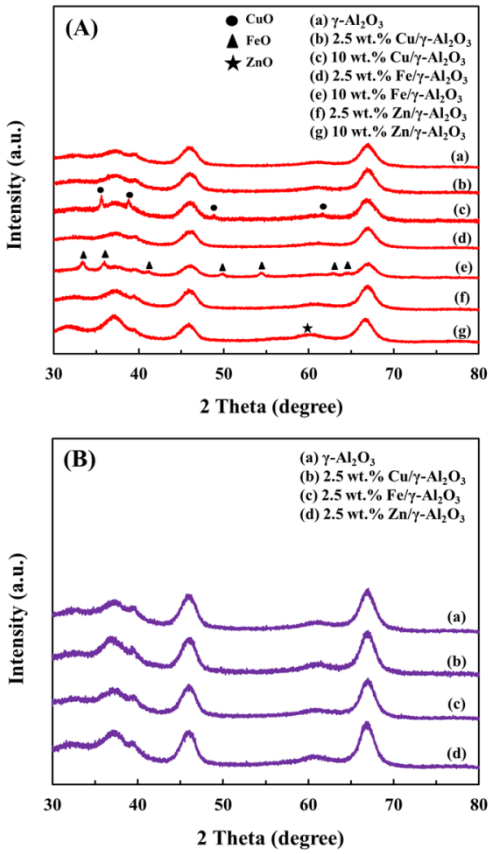

Fig. 1 XRD patterns of (A) catalysts before reaction and (B) catalysts after reaction.

Fig. 2 shows the morphologies of the catalysts, which also indicate that no bulk metal oxide particles are formed on the surface of γ-Al_2O_3 and homogeneously dispersed on the catalyst surface. Fig. 2D-F show metal element mappings on the catalysts. One can clearly see that Cu, Fe and Zn elements have good dispersion without accumulation on surface of γ-Al_2O_3. Fig. 3 shows NH_3-TPD profiles of catalysts. For pure γ-Al_2O_3, NH_3 desorbs at low temperature range of 150 to 500 °C as well as high temperature range of 500 to 780 °C. It is believed that the peaks at low temperature range and high temperature range correspond to the weak acid sites and the strong acid sites, respectively.[38]

Table 2 Physicochemical properties of as-prepared catalysts.

Sample	Surface area (m^2/g)	Pore volume (cm^3/g)	Pore diameter (nm)	Acidity (mmol/g)	Metal content (%)	Metal content after reaction (%)
γ-Al_2O_3	232	0.72	8.97	0.355	-	-
2.5 wt.% Cu/γ-Al_2O_3	202	0.69	7.40	0.359	2.44	2.16
2.5 wt.% Fe/γ-Al_2O_3	189	0.60	8.22	0.367	2.48	2.45
2.5 wt.% Zn/γ-Al_2O_3	190	0.65	8.92	0.428	2.50	2.47
SiO_2	200	0.81	9.04	0.093	-	-
2.5 wt.% Cu/SiO_2	190	0.72	8.97	0.183	-	-
2.5 wt.% Fe/SiO_2	185	0.69	8.98	0.122	-	-
2.5 wt.% Zn/SiO_2	193	0.77	9.03	0.180	-	-

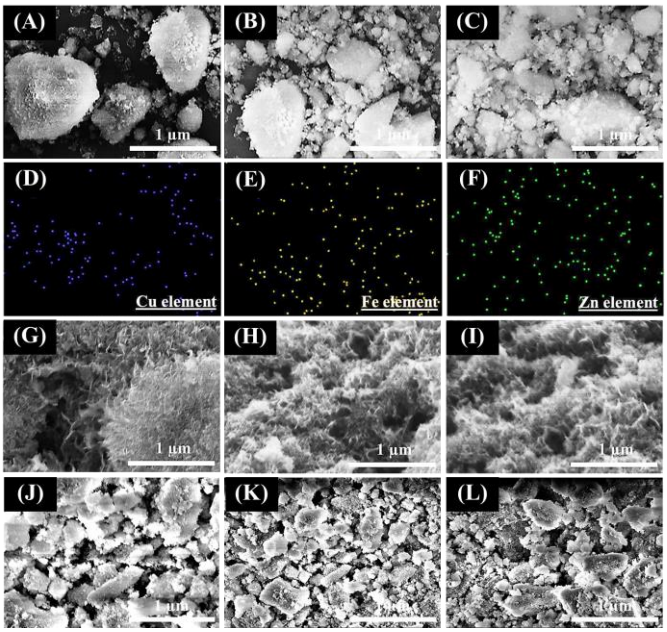

Fig. 2 SEM and EDX mapping images of (A,D) 2.5 wt.% Cu/γ-Al_2O_3, (B,E) 2.5 wt.% Fe/γ-Al_2O_3 and (C,F) 2.5 wt.% Zn/γ-Al_2O_3 catalysts before reaction, SEM images of (G) 2.5 wt.% Cu/γ-Al_2O_3, (H) 2.5 wt.% Fe/γ-Al_2O_3 and (I) 2.5 wt.% Zn/γ-Al_2O_3 catalysts after reaction (without regeneration), (J) 2.5 wt.% Cu/γ-Al_2O_3, (K) 2.5 wt.% Fe/γ-Al_2O_3 and (L) 2.5 wt.% Zn/γ-Al_2O_3 catalysts after reaction (after regeneration).

Interestingly, after the metal is loaded on γ-Al_2O_3, the peak corresponding to the strong acid sites is shifted to the higher temperature due to some interaction occurring between metal and γ-Al_2O_3. The acidities of catalysts are summarized in Table 2. It indicates that when metal is loaded on γ-Al_2O_3, the acidity of catalyst can be promoted. Herein, it should be noted that 2.5 wt.% Zn/γ-Al_2O_3 exhibits higher acidity than other catalysts. Such a high acidity can play an importance role in conversion of oxygenated compounds in bio-oil to hydrocarbons.

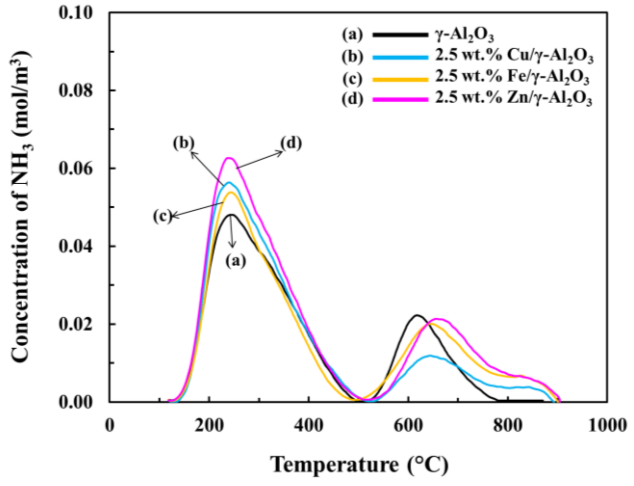

Fig. 3 NH_3-TPD profiles of catalysts.

Table 3 Product yields (wt.%) obtained from pyrolysis of untreated and ultrasonic pretreated cedars.

Biomass	Bio-oil (wt.%)	Water (wt.%)	Gas (wt.%)	Char (wt.%)
Untreated cedar	45.14	17.03	12.50	25.33
Treated cedar	55.60	10.36	13.21	20.83

3.2 Effect of ultrasonic pretreating of cedar on bio-oil yield

Table 3 shows the yields of products including bio-oil, water, gas and char obtained from the pyrolysis of ultrasonic pretreated and untreated cedar. One can see that the yield of bio-oil derived from the pretreated cedar increases about 10 % when compared with that from untreated one. By ultrasonic pretreatment, some long chain units and C-C network could be broken so that the cedar can be more easily pyrolyzed and more bio-oil is obtained. It is reported that by ultrasonic pretreatment, the crystallinity of cellulose can decreased, some bonds in lignin, cellulose and hemicellulose broken, leading to open structures of biomass, which could promote the pyrolysis efficiency.[39] Furthermore, one can see that the yield of gas is also slightly increased from 12.5 to 13.2% after the cedar is pretreated by ultrasound while those of water and char are decreased about 6%.

Fig.4 shows chemical compositions in the bio-oils derived from the pyrolysis of ultrasonic pretreated and untreated cedar. Interestingly, more sugar and ketone compounds, which should be resulted from the cleavage of glycosidic bonds and β-alkyl-aryl bond in biomass, are obtained in the bio-oil from ultrasonic pretreated cedar.[40] Shi *et al.*[41] suggested the possible mechanism for ultrasonic pretreating of biomass. Herein, ultrasound can crack the O-H bond in water molecule to produce hydroxyl and hydrogen radicals (H_2O → •OH + •H), which can attack the chains in biomass, resulting in more radicals and oxidizing species such as ozone and hydrogen peroxide. These oxidizing species could lead to the destruction of firm lignin structure, releasing more cellulose and hemicellulose from biomass structure.

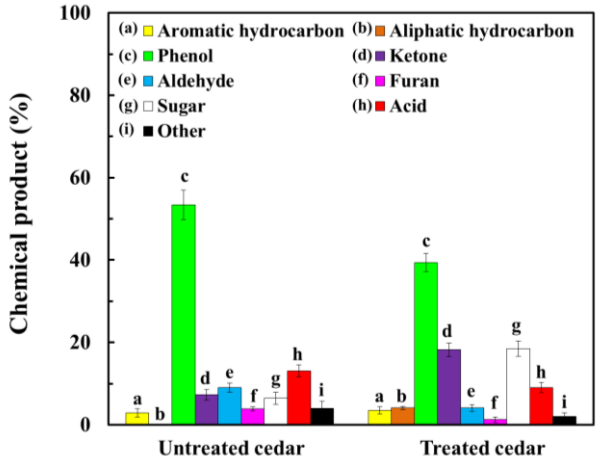

Fig. 4 Chemical compositions in the bio-oils obtained from pyrolysis of untreated and ultrasonic pretreated cedar.

To confirm the change of cedar structure after ultrasonic pretreatment, FT-IR spectra of the pretreated and untreated cedars were measured and the results are shown in Fig. 5. Here, the wavenumber range of 3700-3000 cm^{-1} attributes to –OH stretching vibration of phenolic, alcoholic and carboxylic functional groups. One can see that the peak intensities corresponding to cellulose at the wavenumber range of 3000-2800 cm^{-1} increase to some extent for the pretreated cedar. Likewise, the peak intensities of hemicellulose at 1730 cm^{-1} and lignin at 1595 cm^{-1} are also changed, indicating that ultrasonic pretreatment splits the bind of lignin and makes more cellulose and hemicellulose exposed, leading to an increase of bio-oil yield with the change of some chemical compositions. Unfortunately, this pretreating way cannot improve the quality of bio-oil due to the presence of many oxygenated compounds. As we know, oxygenated compounds such as ketones, phenols and sugars in the bio-oil result in the instability and low heating value of bio-oil; high amount of acid oxygenated compounds leads to the corrosive and other drawbacks such as promoting the adol reaction to accelerate the ageing of bio-oil when it is used in a practical process. Therefore, the obtained bio-oil needs to be upgraded.

3.3 Catalytic upgrading bio-oil from ultrasonic pretreated cedar

Fig. 6A shows chemical compositions of bio-oils upgraded by various catalysts. Herein, the chemical products are classified into nine groups, including aromatic hydrocarbons, aliphatic hydrocarbons, phenols, ketones, aldehydes, furans, sugars, acids and other. Among them, the total relative amount of aromatic hydrocarbons, aliphatic hydrocarbons in the bio-oil is considered as the most important indicator to determine the upgrading effectivity by the catalysts. One can see that the hydrocarbon yield is increased from 2.9 to 35.1% when γ-Al_2O_3 is used. After 10 wt.% metal is loaded on γ-Al_2O_3 and used for bio-oil upgrading, the hydrocarbon yield increases significantly, especially, more aromatic hydrocarbons are formed. For all 10 wt.% metal loaded γ-Al_2O_3 catalysts, they increase the hydrocarbon yields to about 60 %. However, it should be noted that the yield of bio-oil is decreased to some extent when the catalyst is used. It is due to that some oxygenated compounds are converted to water, gas and carbonaceous residue in the presence of catalyst, which can be observed from their increasing yield.

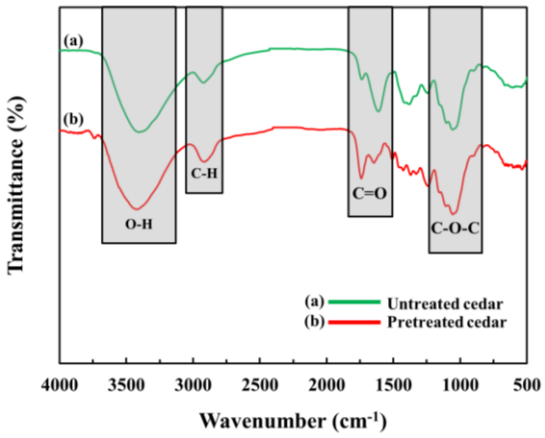

Fig. 5 FT-IR spectra of untreated and ultrasonic pretreated cedar.

Here, sugars are completely converted by using the catalysts for cedar. It is reported that levoglucosan, which is a main chemical in sugar family in bio-oil, can be deoxygenated via two steps as follows: (I) levoglucosan can be converted into furans via dehydration reaction and then, (II) aromatic hydrocarbons can be generated continuously by converting the furans via dehydration and decarboxylation reactions.[24] Meanwhile, the acids can be converted via decarboxylation and decarboxylation reactions, resulting in the formation of CO and CO_2. Fig. 6B and C show product distribution and the yields of various gases, respectively. One can see that the yields of water, carbon monoxide and carbon dioxide increase with the increase in hydrocarbon yield and the decrease in oxygenated compound amount in bio-oil, suggesting that some reactions such as decarboxylation, decarbonylation, oligomerization, isomerization, dehydration and dehydrogenation occur during the catalytic upgrading process.[42]

The effect of metal loading amount on the upgrading effectivity is studied by using various Fe loading amount (1, 2.5, 5 and 10 wt.%) on γ-Al_2O_3. As shown in Fig. 7, the hydrocarbon yield is increased from 55.6 to 68.6 % with the increase in Fe loading amount from 1 to 2.5 wt.% on γ-Al_2O_3, and then the hydrocarbon yield decreased to 6% when Fe loading amount is increased to 10 wt.%. It indicates that the catalytic performance for the conversion of oxygenated compounds into hydrocarbons becomes worse when overloading of Fe on γ-Al_2O_3. When the metal loading amount exceeds its saturation loading point of metal on support, sintering of metal could be easily occurred during the thermal calcination process. Moreover, at higher metal loading amount, surface area and pore size of catalyst are generally decreased, and in this case, the pore blockage occurs due to the low dispersion and high accumulation of metal species, leading to the decreasing of mass transfer and catalytic activity. The metal modified on γ-Al_2O_3 can lead to the replacement of some proton sites in γ-Al_2O_3 with metal ions, by which some new Lewis acid sites are produced and resulted in activity change. Therefore, the optimum loading amount of Fe on γ-Al_2O_3 should be 2.5 wt.% in this study. Here, since different kind of metal loadings present the similar catalytic activity trend by an increasing of hydrocarbon with a decreasing of oxygenated compound. Thus, the optimum loading amount of Fe on γ-Al_2O_3 is also applied for Cu and Zn loadings.

Fig.8A shows chemical compositions of upgraded bio-oil by using 2.5 wt.% metal (Cu, Fe and Zn) loaded γ-Al_2O_3. One can see that the hydrocarbon yields are significantly increased when compared with 10 wt.% metal loaded γ-Al_2O_3 (Fig. 7). Especially, by using 2.5 wt.% Zn/γ-Al_2O_3, the highest hydrocarbon yield of 80.3%, which consists the aromatic hydrocarbon of 60.1% and the aliphatic hydrocarbon of 20.2%, is obtained. The best catalytic activity of Zn/γ-Al_2O_3 is attributed to its higher acidity and stronger acid sites than others due to the stronger interaction between Zinc and γ-Al_2O_3. Moreover, it is possible that Zinc species can promote hydrogen transfer during reaction process. For each catalyst, the aromatic hydrocarbon yield over 60% is achieved, suggesting that a suitable metal loading amount on support is required for promoting the deoxygenation to produce more aromatic hydrocarbons. For comparison, 2.5 wt.% metal/SiO_2 is also prepared and applied for the catalytic upgrading bio-oil. As shown in Fig. 8B, metal/SiO_2 shows much lower catalytic activity on upgrading bio-oil. This is because metal/SiO_2 has less acidity which has been confirmed by the results shown in Table 2.

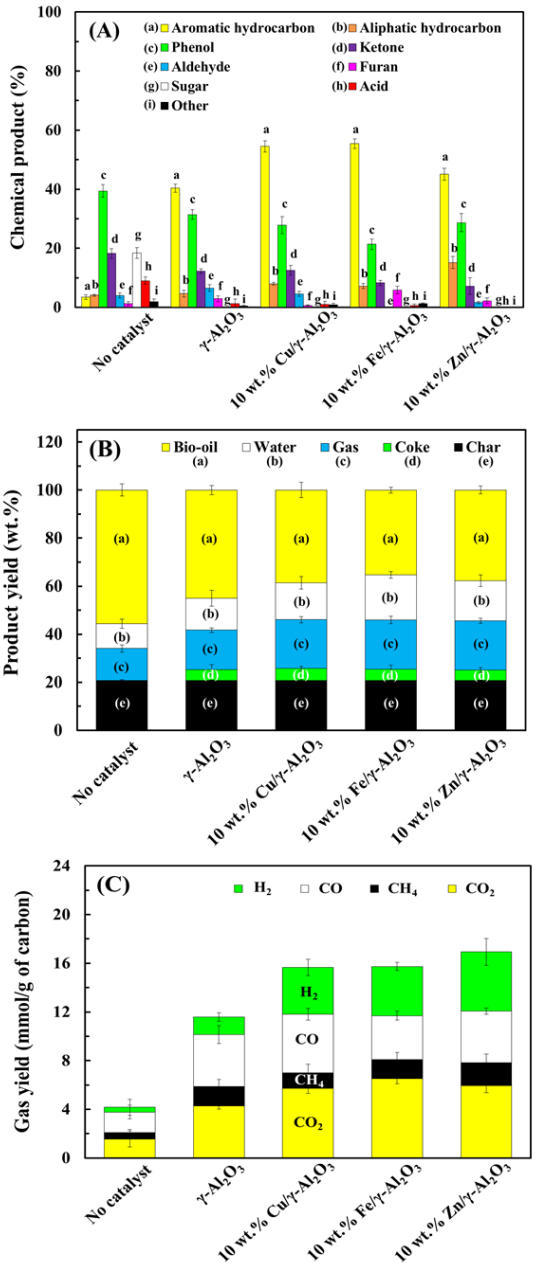

Fig. 6 (A) Chemical compositions in non-upgraded and upgraded bio-oil, (B) mass balance of products and (C) gas yields obtained from in-situ upgrading of bio-oil process on ultrasonic pretreated treated cedar.

Fig. 9 shows the aromatic hydrocarbon distribution in the upgraded bio-oil obtained by using different metal-loaded catalysts. One can see that the amount of monocyclic aromatic hydrocarbons (MAHs) such as benzene, toluene, xylenes, and indenes is much higher than that of polycyclic aromatic hydrocarbons (PAHs) such as naphthalenes, fluorene, phenanthrene and anthracene for any catalysts. The amounts of aromatic compounds in the upgraded bio-oil by using 2.5 wt.% Cu/γ-Al_2O_3 and 2.5 wt.% Fe/γ-Al_2O_3 are in the order of benzene > toluene > naphthalenes > xylenes > indenes > others, while those by using 2.5 wt.% Zn/γ-Al_2O_3 are indenes > benzene > naphthalenes > toluene > xylenes > others. The aromatic hydrocarbons in this study mainly consists of C_5 to C_{12}, as those in gasoline. The obtained benzene, toluene and xylene (BTX) here are the major petrochemical compounds for increasing the octane values in gasoline or used as other fuel precursors.[43] The naphthalene obtained here is probably from the further polymerization of MAHs.

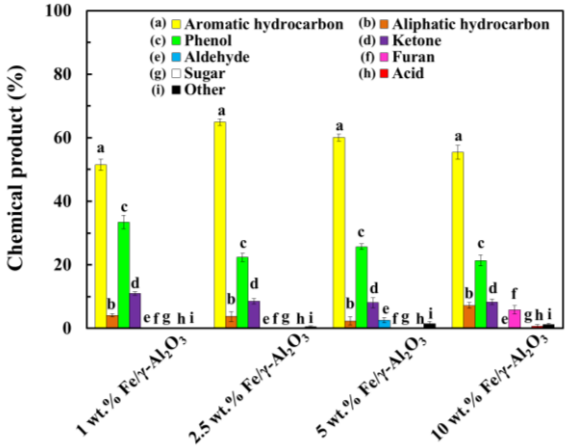

Fig. 7 Effect of Fe loading amount on γ-Al_2O_3 for its catalytic activity on upgrading bio-oil derived from the pyrolysis of ultrasonic pretreated cedar.

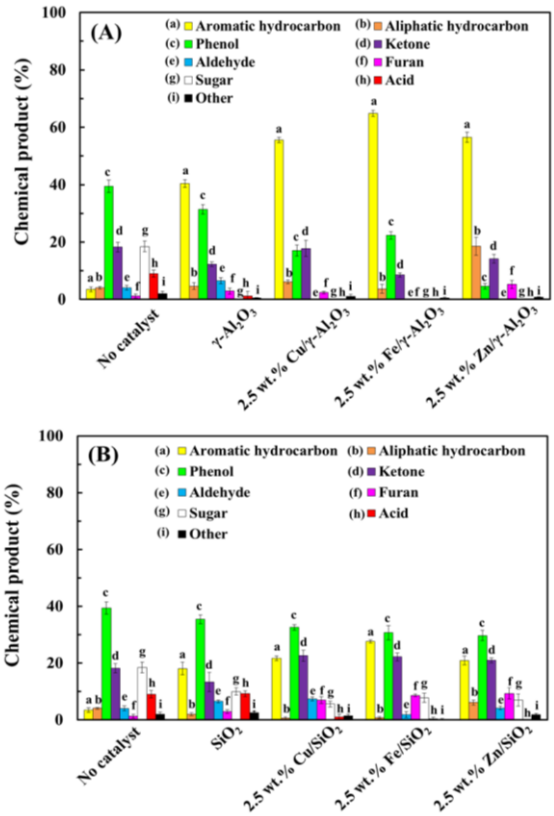

Fig. 8 Chemical compositions in the non-upgraded and upgraded bio-oils obtained from the pyrolysis of ultrasonic pretreated cedar by using (A) metal/γ-Al_2O_3 catalyst and (B) metal/SiO_2 catalyst.

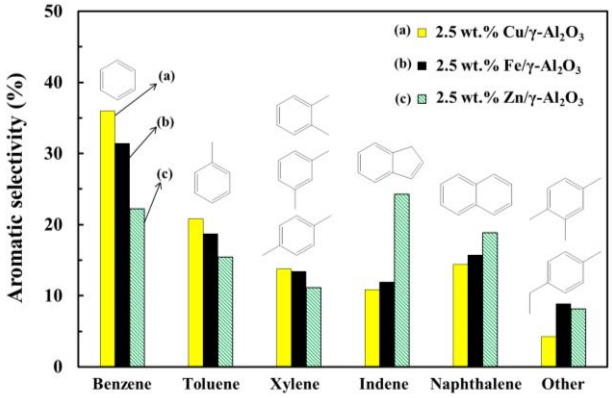

Fig. 9 Aromatic selectivity obtained from upgrading bio-oils derived from the pyrolysis of ultrasonic pretreated cedar using various catalysts.

A possible mechanism by using the metal/γ-Al_2O_3 catalyst for upgrading bio-oil from the pyrolysis of pretreated cedar is proposed as illustrated in Fig. 10. The reactions occurred in the reactor include three cases: (I) within the solid biomass, (II) within the catalyst and (III) in the gas phase. For cellulose, it can be decomposed and dehydrated to form anhydrosugars such as levoglucosan, and then dehydration of levoglucosan occurs and results in the formation of furans[44]. At the same time, hemicellulose can be cleaved at the rings between C_2-C_5 and the bonds between O-C_5, transforming into the furfural which can be converted into the furan through decarbonylation. For lignin, C-C and C-O bonds can be broken and converted to the phenols and phenol alkoxy species.[45,46] In the catalyst layer, aromatics, light olefins, coke and gases are generated by conversion of furan, phenol and low molecular oxygenated compounds, depending on their diffusion on the surface and in the pores of catalyst. Thus, high surface area and large pore size of catalyst can promote efficiently mass transfer of the chemicals in bio-oil and provide more th active sites for the catalytic reactions. Herein, the char can be also produced from polycondensation of aromatics, furans and pheno In this process, the major negative reaction with aromatic production over heterogeneous catalyst is the coke formation on

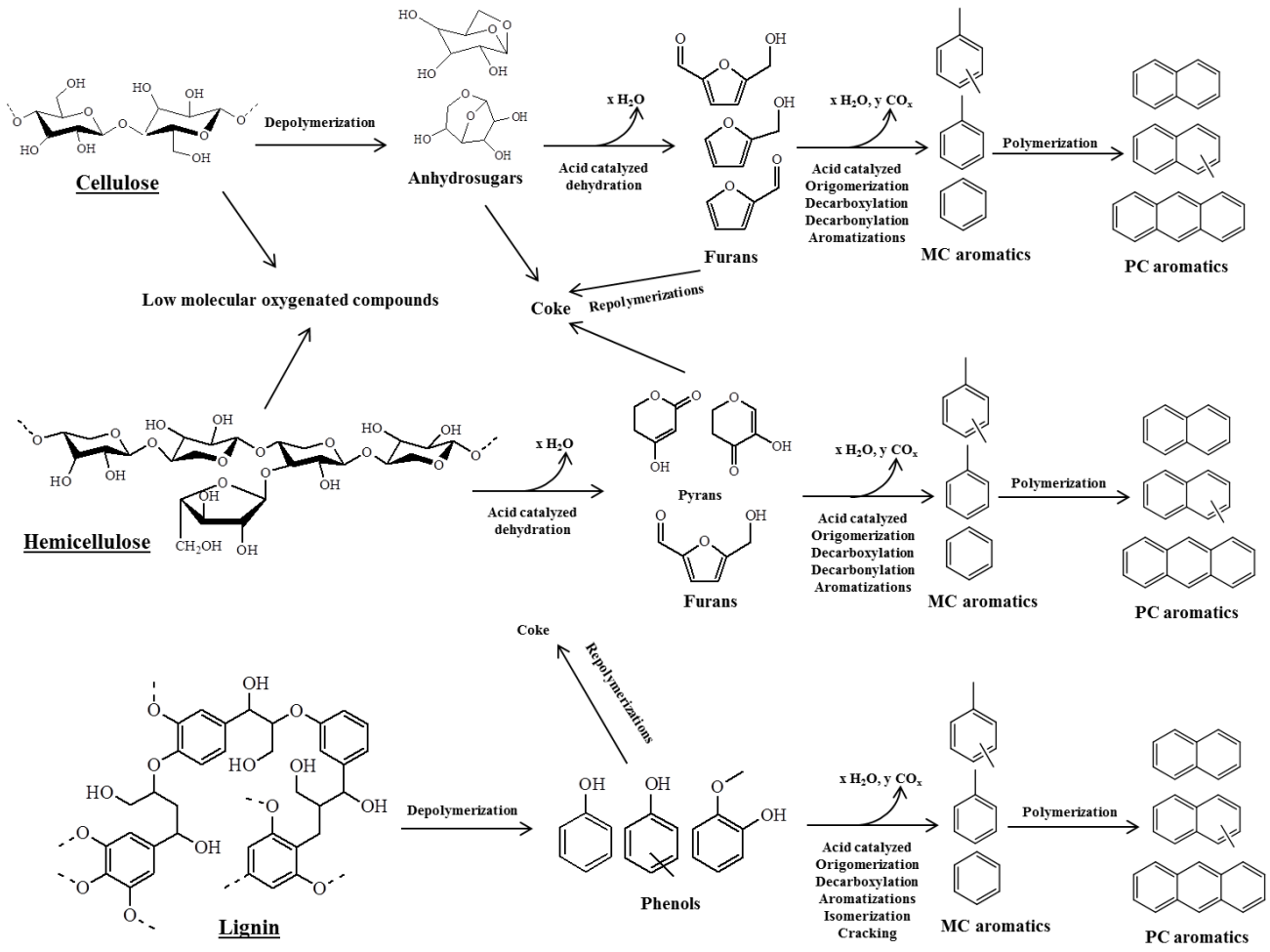

Fig. 10 Reaction mechanisms leading to aromatic compounds by catalytic upgrading of bio-oil from the pyrolysis of biomass.

the catalyst, which can be easily generated from (I) direct thermal decomposition of biomass, (II) by heterogeneously catalyzed reactions and (III) by reactions in the gas phase.[47]

3.4 Catalyst reusability

Due to the coke formation on the catalyst, the activity always decreases after a period reaction. In this study, the spent catalysts, i.e., 2.5 wt.% Cu/γ-Al_2O_3, 2.5 wt.% Fe/γ-Al_2O_3 and 2.5 wt.% Zn/γ-Al_2O_3, are regenerated by calcination of them at 550 °C in air atmosphere for 30 min. Long-term stability of catalysts after regeneration and without regeneration are compared by reuse of them up to 4 cycles. As shown in Fig. 11, one can see that a significant reduction in catalytic performance occurs in each cycle for the spent catalyst without regeneration due to coke deposition on catalyst, which can lead to the coverage of active sites and blockage of pores in catalyst.[48] Here, 2.5 wt.% Cu/γ-Al_2O_3 shows the lowest reusability, which should be resulted from the coke deposition amount and/or Cu metal leaching. As shown in Table 2, metal content on catalyst surface after the reaction decreased to some extent, especially in 2.5 wt.% Cu/γ-Al_2O_3. It is probably due to the weaker interaction between metal and support. However, after the regeneration, only a slight reduction of total hydrocarbon is observed in each cycle, indicating that the catalytic activity is recovered.

Fig. 2G-I show SEM images of spent catalysts (4th reuse) without regeneration. One can see that the carbon filaments are obviously formed on the surfaces of all spent catalysts. However, after the regeneration (Fig. 2J-L), the carbon filaments disappear. The amounts of coke deposition on spent catalysts (4th reuse) are shown in Table 4. The lowest amount of coke deposition is found on Zn/γ-Al_2O_3. It is possible that Zn species could promote hydrogen atom migration through C-H activation which helps to catalyze the oligomerization of intermediates during pyrolysis reaction, leading to the preservation and the improving stability of catalyst by preventing coke deposition on the surface of catalyst.[35] Recently, Fanchiang and Lin[49] found that the oxygenated compounds can be well converted into hydrocarbon, especially, benzene by using Zn/H-ZSM-5. They also considered that Zn species can play an important role in hydrogen atom transfer, leading to the change of acid site concentration. From these results, we can conclude that Zn loaded γ-Al_2O_3 is an interesting catalyst for upgrading of bio-oil and can be potentially applied for a practical process.

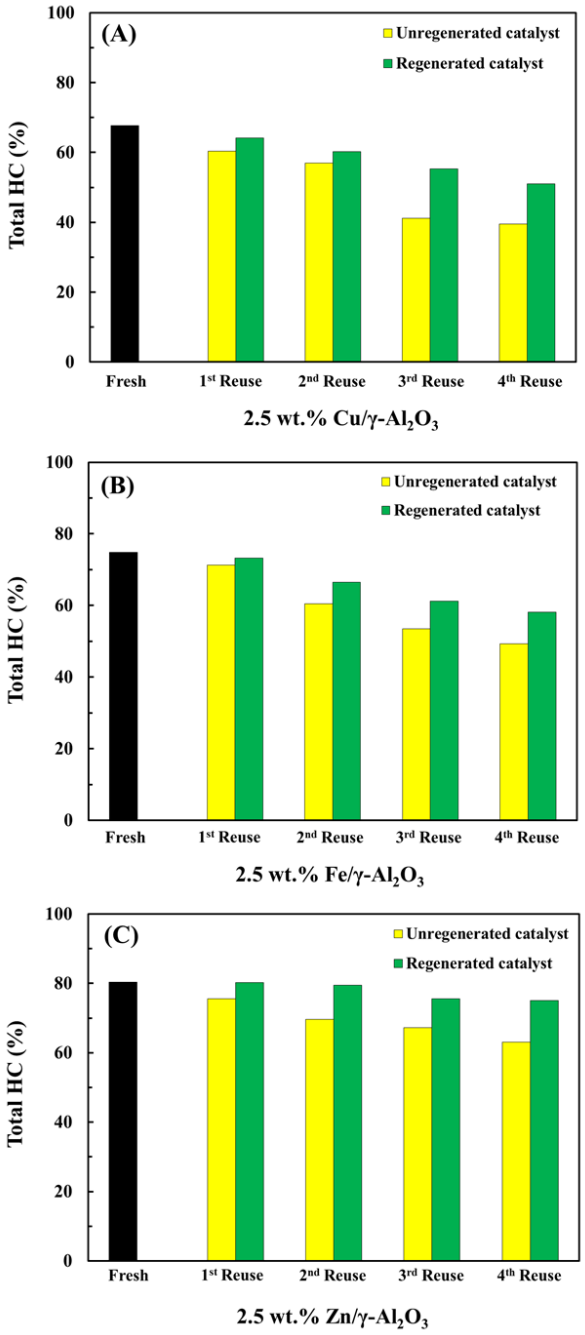

Fig. 11 Catalyst reusability of (A) 2.5 wt.% Cu/γ-Al_2O_3, (B) 2.5 wt.% Fe/γ-Al_2O_3 and (C) 2.5 wt.% Zn/γ-Al_2O_3 for catalytic upgrading of bio-oil derived from the pyrolysis of ultrasonic pretreated cedar.

Table 4 The amount of coke deposition on catalyst after reaction (4th reuse)

Spent catalyst	Coke deposition (%)
2.5 wt.% Cu/γ-Al_2O_3	9.81
2.5 wt.% Fe/γ-Al_2O_3	8.72
2.5 wt.% Zn/γ-Al_2O_3	7.98

Fig. 12 shows DTG thermograms of spent catalysts (4th reuse). The derivative weight loss peak of catalyst appeared at the temperature range of about 350 to 550 °C. The different decomposition temperature ranges should be due to the different carbon particle sizes and different carbon deposition positions on catalysts.[50,51] It should be noted that even though the decomposition temperature range for coke removal from Zn/γ-Al_2O_3 is higher than those for other catalysts, there is no effect on its catalytic activity for upgrading of bio-oil.

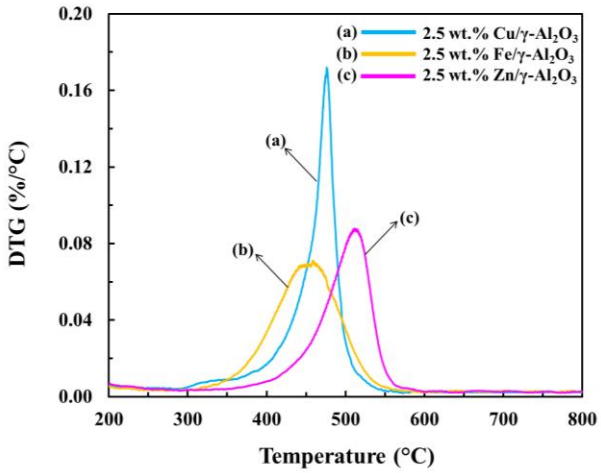

Fig. 12 DTG curves of catalysts after reaction (4th reuse).

4 Conclusions

Ultrasonic pretreatment of cedar is a suitable way to increase the bio-oil yield but it cannot improve the bio-oil quality. Upgrading bio-oil derived from the cedar pyrolysis is achieved by using metal (Cu, Fe and Zn) loaded γ-Al_2O_3 catalysts. It is found that 2.5 wt.% of metal loading amount is the optimum for the present study. Especially, 2.5 wt.%Zn/γ-Al_2O_3 exhibits the highest catalytic activity and long-term stability for conversion of oxygenated compounds to hydrocarbons. It is related to its acidity and coking resistance properties when comparing with other metal loaded γ-Al_2O_3 catalysts. It is expected that the yield of bio-oil together with its quality can be promoted by using this green process.

Acknowledgements

This study is supported by Strategic International Collaborative Research Program (SICORP), Japan Science and Technology (JST), Aomori city government, Japan, and the International Joint Research Project of Shanxi Province (No.2015081051and 2015081052）. S. Karnjanakom, and B. Asep greatly acknowledge the Ministry of Education, Culture, Sports, Science, and Technology (MEXT) of Japan for the scholarship.

References

1 S. Ren, H. Lei, L. Wang, Q. Bu, S. Chen, J. Wu, J. Julson and R. Ruan, *Bioresour. Technol.*, 2013, **135**, 659–664.
2 J. Lehto, A. Oasmaa, Y. Solantausta, M. Kytö and D. Chiaramonti, *Appl. Energy*, 2014, **116**, 178–190.
3 D. Shen, R. Xiao, S. Gu and K. Luo, *RSC Adv.*, 2011, **1**, 1641–1660.
4 M. Asadieraghi, W. M. A. W. Daud and H. F. Abbas, *RSC Adv.*, 2015, **5**, 22234–22255.
5 M. Cordella, C. Torri, A. Adamiano, D. Fabbri, F. Barontini and V. Cozzani, *J. Hazard. Mater.*, 2012, **231–232**, 26–35.
6 M. S. Singhvi, S. Chaudhari and D. V. Gokhale, *RSC Adv.*, 2014, **4**, 8271–8277.
7 M. Mohan, T. Banerjee and V. V. Goud, *Bioresour. Technol.*, 2015, **191**, 244–252.
8 S. Kumagai, R. Matsuno, G. Grause, T. Kameda and T. Yoshioka, *Bioresour. Technol.*, 2015, **178**, 76–82.
9 J. Akhtar and N. A. S. Amin, *Renewable Sustainable Energy Rev.*, 2011, **15**, 1615–1624.
10 A. Ranjan and V. S. Moholkar, *Fuel*, 2013, **112**, 567–571.
11 R. Yunus, S. F. Salleh, N. Abdullah and D. R. A. Biak, *Bioresour. Technol.*, 2010, **101**, 9792–9796.
12 X. Ying, W. Tiejun, M. Longlong and C. Guanyi, *Energy Convers. Manage.*, 2012, **55**, 172–177.
13 S. Vitolo, M. Seggiani, P. Frediani, G. Ambrosini and L. Politi, *Fuel*, 1999, **78**, 1147–1159.
14 Y. Wang, J. Wu and S. Wang, *RSC Adv.*, 2013, **3**, 12635–12640.
15 P. S. Rezaei, H. Shafaghat and W. M. A. W. Daud, *Appl. Catal., A*, 2014, **469**, 490–511.
16 J. A. Capunitan and S. C. Capareda, *Fuel Process. Technol.*, 2014, **125**, 190–199.
17 Z. Qi, C. Jie, W. Tiejun and X. Ying, *Energy Convers. Manage.*, 2007, **48**, 87–92.
18 A. Veses, B. Puértolas, M. S. Callén and T. García, *Microporous Mesoporous Mater.*, 2015, **209**, 189–196.
19 E. Kantarelis, W. Yang and W. Blasiak, *Fuel*, 2014, **122**, 119–125.
20 W. B. Widayatno, G. Guan, J. Rizkiana, X. Du, X. Hao, Z. Zha[illegible] and A. Abudula, *Bioresour. Technol.*, 2015, **179**, 518–523.
21 F. Yu, L. Gao, W. Wang, G. Zhang and J. Ji, *J. Anal. Appl. Pyrolysis*, 2013, **104**, 325–329.
22 Q. Lu, Z. Zhang, X. Wang, C. Dong and Y. Liu, *Energy Procedia*, 2014, **61**, 1937–1941.
23 Y. Xu, T. Wang, L. Ma, Q. Zhang and W. Liang, *Appl. Energy*, 2014, **87**, 2886–2891.
24 D. J. Mihalcik, C. A. Mullen and A. A. Boateng, *J. Anal. Appl. Pyrolysis*, 2011, **92**, 224–232.
25 Q. Lu, Y. Zhang, Z. Tang, W. Li and X. Zhu, *Fuel*, 2010, **89**, 2096–2103.
26 P. Kaewpengkrow, D. Atong and V. Sricharoenchaikul, *Bioresour. Technol.*, 2014, **163**, 262–269.
27 S. Stephanidis, C. Nitsos, K. Kalogiannis, E. F. Iliopoulou, A. [illegible] Lappas and K. S. Triantafyllidis, *Catal. Today*, 2011, **167**, 37–45.
28 E. Antonakou, A. Lappas, M. H. Nilsen, A. Bouzga and M. Stöcker, *Fuel*, 2006, **85**, 2202–2212.
29 W. Liu, K. Tian, H. Jiang, X. Zhang, H. Ding and H. Yu, *Environ. Sci. Technol.*, 2012, **46**, 7849–7856.
30 F. X. Collard, J. Blin, A. Bensakhria and J. Valette, *J. Anal. Appl. Pyrolysis*, 2012, **95**, 213–226.
31 Y. Shen, C. Areeprasert, B. Prabowo, F. Takahashi and K. Yoshikawa, *RSC Adv.*, 2014, **4**, 40651–40664.
32 C. Liu, H. Wang, A. M. Karim, J. Sun and Y. Wang, *Chem. Soc. Rev.*, 2014, **43**, 7594–7623.
33 R. French and S. Czernik, *Fuel Process. Technol.*, 2010, **91**, 25–32.
34 A. Imran, E. A. Bramer, K. Seshan and G. Brem, *Fuel Process. Technol.*, 2014, **127**, 72–79.
35 L. Wang, H. Lei, Q. Bu, S. Ren, Y. Wei, L. Zhu, X. Zhang, Y. Liu, G. Yadavalli, J. Lee, S. Chen and J. Tang, *Fuel*, 2014, **129**, 78–85.
36 M. Kaewpanha, G. Guan, X. Hao, Z. Wang, Y. Kasai, K. Kusakab[illegible] and A. Abudula, *Fuel Process. Technol.*, 2014, **120**, 106–112.
37 T. P. Braga, A. N. Pinheiro, E. R. Leite, R. C. R. Santos and A. Valentini, *Chin. J. Catal.*, 2015, **36**, 712–720.
38 D. L. Hoang, T. T. H. Dang, J. Engeldinger, M. Schneider, [illegible] Radnik, M. Richter and A. Martin, *J. Solid State Chem.*, 2011, **184**, 1915–1923.
39 M. J. Bussemaker and D. Zhang, *Ind. Eng. Chem. Res.*, 2013, **52**, 3563−3580.

40 S. Li, J. Lyons-Hart, J. Banyasz and K. Shafer, *Fuel*, 2001, **80**, 1809–1817.

41 W. Shi, J. Jia, Y. Gao and Y. Zhao, *Bioresour. Technol.*, 2013, **146**, 355–362.

42 S. Vichaphund, D. Aht-ong, V. Sricharoenchaikul and D. Atong, *Renewable Energy*, 2015, **79**, 28–37.

43 T. R. Carlson, Y. Cheng, J. Jae and G. W. Huber, *Energy Environ. Sci.*, 2011, **4**, 145–161.

44 M. S. Mettler, A. D. Paulsen, D. G. Vlachos and P. J. Dauenhauer, *Energy Environ. Sci.*, 2012, **5**, 7864–7868.

45 C. Amen-Chen, H. Pakdel and C. Roy, *Bioresour. Technol.*, 2001, **79**, 277–299.

46 Y. Zheng, D. Chen and X. Zhu, *J. Anal. Appl. Pyrolysis*, 2013, **104**, 514–520.

47 J. Jae, G. A. Tompsett, A. J. Foster, K. D. Hammond, S. M. Auerbach, R. F. Lobo and G. W. Huber, *J. Catal.*, 2011, **279**, 257–268.

48 M. Baghalha, M. Mohammadi and A. Ghorbanpour, *Fuel Process. Technol.*, 2010, **91**, 714–722.

49 W. L. Fanchiang and Y. C. Lin, *Appl. Catal., A*, 2012, **419–420**, 102– 110.

50 R. B. Mathur, S. Chatterjee and B. P. Singh, *Compos. Sci. Technol.*, 2008, **68**, 1608–1615.

51 B. Scheibe, E. Borowiak-Palen and R. J. Kalenczuk, *Mater. Charact.*, 2010, **61**, 185–191.